GRAIN-SCALE FIELD DOCUMENTATION OF AEOLIAN TERRESTRIAL ANALOGS USING STEREOPHOTOGRAMMETRY OF MEGARIPPLES AT GREAT SAND DUNES. S. P. Scheidt[1,2,3,4], J. R. Zimbelman[5], M. M. Baker[5]. [1]Howard University, 2400 6th St NW, Washington, DC 20059 (sscheidt77@gmail.com). [2]Planetary Science Institute, Odenton, MD 21113. [3]Solar System Exploration Division, NASA Goddard Space Flight Center, Greenbelt, MD 20771. [4]Center for Research and Exploration in Space Science and Technology, NASA/GSFC, Greenbelt, MD 20771 [5]CEPS/NASM, MRC 315, Smithsonian Institution, Washington, DC 20013-7012.

Introduction: Aeolian bedforms are found on Earth, Mars, Venus and Titan. In this research, we are interested in the complex interaction of sand ripples and megaripples that reflect different modes of sediment transport. Sand-sized particles are moved by saltation and coarse-grains are moved via impact creep. Previous remote sensing studies have focused on the aeolian mobility of sand on Mars [1] using High Resolution Imaging Science Experiment (HiRISE [2]). These images documented that sand is moving at many locations under current conditions [3-5]. In particular, Mars has an intriguing conglomeration of active and inactive aeolian bedforms that coincide in the same environment. These include sand ripples, megaripples and dunes. Among these are Transverse Aeolian Ridges (TARs; the non-genetic term for linear to curvilinear aeolian bedforms resulting from either dune- or ripple-forming processes [6]). They are widely distributed across Mars [7-9] and were recently documented to also have moved in HiRISE images [10]. Curiosity rover images show that ripples of multiple sizes and wavelengths are common [11-14], but at the field scale, digital topography of the martian surface is not available from rovers or remote sensing. Therefore either terrestrial analog studies [15] or physics-based models [16] are needed to describe how these systems evolve and interact.

Here, we describe the field methodology, capability and results from the first test in the field using specialized camera rigging designed for this project. We captured a very high spatial resolution digital terrain model (DTM) that quantitatively reveals complex superimposed aeolian patterns down to the granule scale of megaripples. These data presented here were collected from a megaripple at Great Sand Dunes National Park and Preserve (GSDNPP) in Colorado [17] funded by a Smithsonian Scholarly Studies Award.

Field Methodology: A specialized camera rig was designed and built for the purpose of collecting image data in the field of natural sand surface. There images are used to produce DTMs and color image orthomosaics using multiview stereo photogrammetry (MVSP) software (Agisoft Metashape). The basic construction of the rig is a motorized camera dolly on a 1.5 m length of rails suspended between two tripods using custom 3D-printed fixtures, where the camera is mounted to view an area perpendicular to the sand surface at ~1.15 m above the ground (Fig. 1). Images are acquired from several 100s to 1000s of viewpoints of the ground target in a grid pattern. The camera, a Nikon D7100 with a 24 MP sensor, travels the rails and automatically takes overlapping pictures a few seconds apart in the "X" direction. The entire rig is manually advanced along a transect in the "Y" direction, perpendicular to the travel of the camera on the rail to build up overlapping images. Dice (15 mm per side) were places in the field of view for scale.

Figure 1. A field macro stereophotogrammetry rig.

3D points are reconstructed by the software from the correlation and triangulation of features. Calculations are complex and require a computer with adequate memory, CPU and GPU resources. The software simultaneously computes projection matrices of the camera for each image, including exact interior (focal length, principle point and lens distortion coefficients) and exterior camera orientation (position-al x, y and z and rotations κ, φ and ω) parameters for each image and a set of 3D points. Images need to have sufficient spatial resolution so that unique features are detected and matched from multiple overlapping images.

Depending on the camera field of view (FOV), this is challenging because sandy surfaces are generally homogenous or "look alike" and matching results could be poor without exact alignment. A 35 mm lens on the Nikon D7100 has a diagonal FOV of 44.1° and produced exceptional results because of sufficient image overlap and footprint size (~0.75 × 0.5 m). The footprint of an 85 mm lens however only has a FOV of 18.9° and a 0.3 × 0.2 m footprint. The specialized camera rig is needed to produce systematically overlapping images for MVSP. The resulting image pixel size at the sand surface using this system is ~50 microns. A dense reconstruction of the scene produces color-textured, to-scale 3D models which were analyzed in CloudCompare and a geographic information system (GIS).

Data Analysis: The high resolution 3D model contained roughly 370 million 3D points. Each 3D point has

photographic color values (RGB), location (XYZ) and a normal vector indicating direction of the 3D surface. This data were downsampled to a regular grid of 200 million for analysis. Topography data were decomposed based on a range of length scales or kernels (k) between 0.1 mm and 20 mm. The roughness tool in CloudCompare was used to calculate topographic height (H) above the sand bed along small length scales (k = 0.1, 0.25, 0.5, 1, 2 and 2.5 mm). k is specified as the radius of a sphere centered on each 3D data point, and H for each 3D point is calculated as the distance between this point and the best fitting plane computed on its nearest neighbors within the kernel size k. Larger kernel sizes were too computationally intensive so 3D data was resampled and "meshed" at k = 5, 10 and 20 mm. Each point H was then calculated as the C2 distance between the 3D point and the interpolated mesh (gridded at 0.1 mm).

k (mm)	Relief (mm)	Mean H (mm)	σ (mm)
0.10	0.09	0.01	0.005
0.25	0.21	0.02	0.01
0.50	0.36	0.04	0.03
1.00	0.78	0.06	0.04
2.00	1.14	0.07	0.06
2.50	1.27	0.08	0.06
5.00	6.95	4.17	0.19
10.0	8.86	4.29	0.25
20.0	21.4	14.9	0.50
DEM	82.5	35.1	15.5

Table 1. Statistics of average height above surface (H), relief and standard deviation (σ) for different length scales (k).

Preliminary Results: A summary of statistics of the results are presented in Table 1. Image maps of scale-dependent patterns are shown in Fig. 2. The data clearly resolves the megaripple, superimposed impact ripples and the individual coarse (1-2-mm diameter) particles on the bedforms, providing a detailed record of the surface distribution of coarse grains across both sand ripple and megaripple bedforms. Coarse grains are stacked several particles deep at the crests of megaripples, a condition common on many megaripples [e.g. 18, 19]. Sand ripples and megaripples are two bedform scales that are clearly resolved and their interaction is clearly seen in the overlapping patterns shown at different length scales (Fig. 2). Image overlap can be seen by patterns seen in the noise exacted when k = 0.1 mm.

References: [1] Zimbelman, J. R. (2019) Icarus 333, 127-129, doi: 10.1016/j.icarus.2019.05.017. [2] McEwen, A.S., et al. (2007) JGR-Planets 112, E05S02, doi: 10.1029/2005JE002605. [3] Silvestro, S., et al., (2010) GRL 37, L20203, doi: 10.1016/ j.icarus.2019 05.017. [4] Bridges, N., et al. (2012) Geology 40, 31-34, doi: 10.1130/G32373.1. [5] Banks, M. E., et al. (2018) JGR-Planets 123, 3205-3219, doi:10.1029/2018 JE005747. [6] Bourke, M.C., et al. (2003) LPS XXXIV, Abs# 2090. [7] Wilson, S. A., J. R. Zimbelman (2004) JGR-Planets 109, E10003, 10.1029/2004JE002247. [8] Balme et al., 2008. [9] Berman et al., 2011, 2018. [10] Silvestro, S., et al. (2019) LPS L, Abs# 1800. . [11] Sullivan, R.S., et al. (2005) Nature 436, doi: 10.1038/nature03641. [12] Sullivan, R. S., et al. (2008) JGR-Planets 113, E06S07, doi:10.1029/2008JE003101. [13] Lapotre, M. G. A., et al. (2018) GRL 45, 10,229-10,239, doi: 10.1029/2018GL079029. [14] Baker, M. M., et al. (2018) GRL 45, 8853-8863, doi: 10.1029/2018GL079040. [15] Zimbelman, J. R. (2020), IPDW, Abstract #3031. [16] Vincent, O. D. (2019), Nature Geo., 12(5), 345-350. [17] Madole, R. F., et al. (2008) Geomorph. 99, 99-119. [18] Sharp, R. P. (1963) J. Geol. 71, 617-636. [19] de Silva, S. L., et al. (2013) GSAB 125 (11/12), 1912-1929, doi: 10.1130/B30916.1.

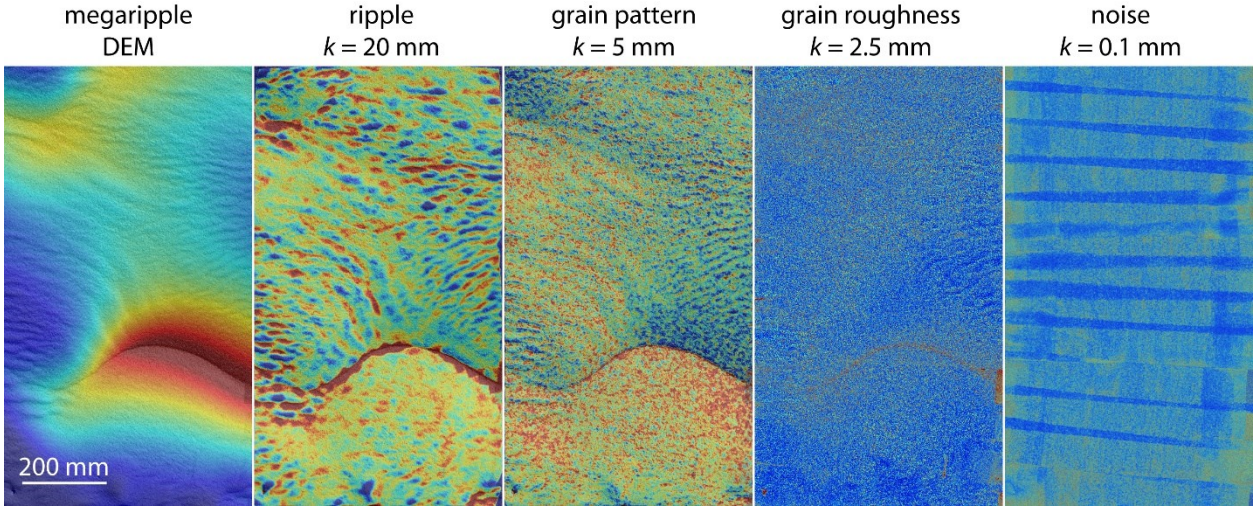

Figure 2. The DTM of the GSDNPP megaripple decomposed into different length scales of topography. Missing from this series is the largest wavelength of topography, the large dunes on which megaripples are superimposed.